Manoyloxide Sesterterpenoids from Salvia mirzayanii

ARTICLE *in* JOURNAL OF NATURAL PRODUCTS · APRIL 2014

Impact Factor: 3.8 · DOI: 10.1021/np400948n · Source: PubMed

JOURNAL OF NATURAL PRODUCTS

Article

pubs.acs.org/jnp

Manoyloxide Sesterterpenoids from *Salvia mirzayanii*

Samad N. Ebrahimi,[†,‡,⊥] M. Moridi Farimani,*[,†,⊥] Foroogh Mirzania,[†] Mohammad A. Soltanipoor,[§] Maria De Mieri,[‡] and Matthias Hamburger*[,‡]

[†]Department of Phytochemistry, Medicinal Plants and Drugs Research Institute, Shahid Beheshti University, G. C., Evin, Tehran, Iran

[‡]Department of Pharmaceutical Sciences, University of Basel, Klingelbergstrasse 50, 4056 Basel, Switzerland

[§]Hormozgan Agricultural and Natural Resources Research Center, Bandarabbas, Iran

Supporting Information

ABSTRACT: Five new manoyloxide-type sesterterpenes were isolated from aerial parts of *Salvia mirzayanii*, a species endemic to Iran. The planar structures were established by means of 1D and 2D NMR and HRESIMS. Compounds **1**−**3** differed only in their configurations at C-13 and C-14. Assignment of relative and absolute configurations was achieved by NOESY experiments and by comparison of experimental and simulated ECD spectra of possible stereoisomers. The absolute configurations of **4** and **5** were established in a similar manner.

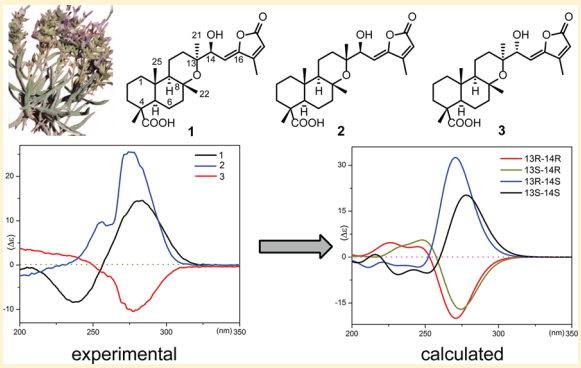

Salvia is the largest genus of the family Lamiaceae and includes over 1000 species distributed throughout the world.[1] A wide range of structurally diverse secondary metabolites have been identified in *Salvia* species, including volatile constituents such as mono- and sesquiterpenes, di-, sester-, and triterpenes, and numerous phenolic constituents.[1] Some *Salvia* species, such as *S. officinalis* or *S. miltiorrhiza*, are of economic importance because of their use as spices, as a source for essential oils, and as medicinal plants. The Iranian flora comprises 58 *Salvia* species, 17 of which are endemic.[2] Some Iranian *Salvia* species have been investigated from a phytochemical viewpoint, and antibacterial, antifungal, antiprotozoal, and antioxidant compounds have been reported.[3−9] The most predominant secondary metabolites in *Salvia* species are terpenoids, and they have been credited for most of the biological activities reported for the genus. The occurrence of sesterterpenoids (C_{25}) in aerial parts is a characteristic feature of the genus *Salvia*.[1,10,11] Sesterterpenoids are more commonly found in marine sponges and algae,[12] and they reportedly possess diverse biological and pharmacological properties, such as anti-inflammatory, cytotoxic, antimicrobial, and antibiofilm activities.[12] Sesterterpenes have been reported from endemic *Salvia* species of Iran, such as *S. hypoleuca*,[13] *S. sahendica*,[14,15] and *S. mirzayanii*.[16] In Iranian folk medicine, the aerial parts of *S. mirzayanii* have been used as a tonic and as a treatment for infectious and inflammatory diseases. The essential oil of *S. mirzayanii* possesses antimicrobial activity, and a new sesterterpenoid has been isolated.[16] In a search for new secondary metabolites from endemic Iranian Lamiaceae,[7−9,15] an acetone extract of *S. mirzayanii* was investigated. Herein is reported the isolation and structure elucidation of five new manoyloxide-type sesterterpenoids from *S. mirzayanii* and the establishment of their absolute configuration by electronic circular dichroism spectroscopy (ECD).

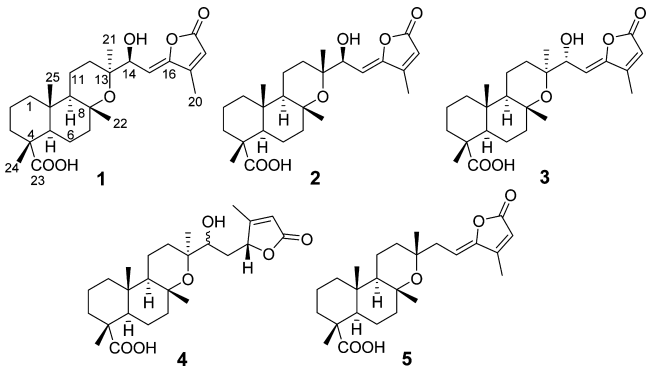

RESULTS AND DISCUSSION

A molecular formula of $C_{25}H_{36}O_6$ for compound **1** was deduced from ^{13}C NMR and HRESIMS data (m/z 455.2399 $[M + Na]^+$; calcd 455.2410), accounting for eight indices of hydrogen deficiency. On the basis of DEPT multiplicities, 25 resonances in the ^{13}C NMR spectrum were assigned to five methyl, seven methylene, five methine, and eight quaternary carbons. Hence, 34 hydrogen atoms could be accounted for, while the remaining two were assigned to hydroxy and carboxylic acid moieties. The ^{13}C NMR spectrum (Table 2) showed resonances for two trisubstituted double bonds (δ_C 151.8, 111.1 and 155.2, 117.1)

Received: November 14, 2013
Published: April 1, 2014

Table 1. ^{1}H NMR Data of Compounds 1−5 ($CDCl_3$ + Methanol-d_4, 500 MHz)

	1	2	3	4	5
position	δ_H (J, Hz)	δ_H (J, Hz)	δ_H (J, Hz)	δ_H (J, Hz)	δ_H (J, Hz)
1	1.04, ddd (14.1, 12.8, 3.1)	1.03, ddd (14.0, 12.0, 3.2)	1.01, ddd (14.0, 12.2, 3.8)	0.94, ddd (14.1, 12.8, 3.1)	1.00 ddd (13.9, 12.6, 3.0)
	1.71	1.70	1.70	1.55	1.67
2β	1.57	1.57	1.54	1.46	1.58
2α	1.67	1.63	1.63	1.55	1.62
3a	1.59	1.62	1.65	1.61	1.62
3b	1.78	1.80	1.80	1.71	1.80
5	1.80	1.77	1.81	1.72	1.82
6β	1.65	1.60	1.63	1.59	1.60
6α	1.59	1.51	1.47	1.44	1.55
7a	1.82	1.75	1.81	1.63	1.78
7b	1.54	1.44	1.53	1.38	1.50
9	1.44	1.17	1.21	1.50	1.35
11α	1.46	1.45	1.47	1.21	1.28
11β	1.33	1.30	1.36	1.32	1.40
12α	1.45	1.49	1.48	1.38	1.56
12β	1.90 ddd (13.7, 5.3, 5.3)	1.82,	1.92 ddd (13.6, 9.2, 4.7)	2.03 ddd (12.6, 10.6, 4.7)	1.81
14a	4.85, d (7.0)	4.48, d (9.4)	4.29, d (9.4)	3.75, d (10.6)	2.52, dd (15.8, 7.2)
14b					2.79, dd (15.8, 6.2)
15a	5.34, d 7.0)	5.23, d (9.4)	5.31, d (9.4)	1.72	5.51, dd (7.2, 6.2)
15b				1.58	
16				5.03, d (10.4)	
18	6.02, brs	5.94, s	5.99, s	5.71, q (1.6)	5.91, s
20	2.17, d (1.0)	2.16, s	2.18, s	2.0, brs	2.17, s
21	1.12, s	1.24, s	1.16	1.05, s	1.16, s
22	1.40, s	1.29, s	1.26	1.12, s	1.28, s
24	1.15, s	1.14, s	1.17, s	1.05, s	1.13, s
25	0.89, s	0.82, s	0.83, s	0.76, s	0.81, s

Table 2. ^{13}C NMR Data of Compounds 1−5 ($CDCl_3$ + Methanol-d_4, 125 MHz)

	1	2	3	4	5
position	δ_C	δ_C	δ_C	δ_C	δ_C
1	38.2	38.2	38.3	38.1	38.7
2	17.5	17.7	17.7	17.3	17.5
3	36.9	37.8	37.1	37.3	37.8
4	46.3	47.4	47.4	46.8	47.2
5	50.5	50.6	50.7	50.6	50.6
6	14.8	15.0	14.5	13.7	15.2
7	42.8	42.7	42.7	43.1	42.7
8	76.9	75.5	76.2	75.7	75.8
9	56.4	58.1	58.5	54.8	57.6
10	36.9	36.4	36.3	36.3	36.9
11	22.5	22.6	24.5	24.0	22.9
12	32.6	33.3	30.7	28.3	37.5
13	77.4	76.0	76.3	75.5	73.4
14	70.3	73.4	73.1	71.3	37.4
15	111.1	110.9	109.5	36.9	110.5
16	151.8	151.4	152.5	82.9	151.7
17	155.2	154.1	154.8	171.1	154.9
18	117.1	117.3	117.5	115.8	116.2
19	169.4	169.3	169.1	174.3	169.9
20	11.7	12.1	12.1	13.6	12.2
21	24.5	23.4	24.5	23.7	31.3
22	24.8	24.6	24.8	25.1	24.4
23	181.7	184.2	184.6	181.5	184.2
24	16.0	16.1	15.9	15.7	15.5
25	15.8	16.0	16.2	14.8	16.8

and two carbonyl carbons (δ_C 169.4, 181.7). Three carbon resonances at δ_C 77.4 (C), 76.9 (C), and 70.3 (CH) indicated that they were linked to oxygen. The absence of other sp and sp^2 carbon resonances implied that compound **1** had to be tetracyclic in order to satisfy eight indices of hydrogen deficiency. The ^{1}H NMR spectrum showed resonances of five methyl groups at δ 2.17 (H_3-20), 1.40 (H_3-22), 1.15 (H_3-24), 1.12 (H_3-21), and 0.89 (H_3-25), one oxymethine at δ 4.85 (H-14, d, J = 7.0), and two vinyl protons at δ 6.02 (H-18, s) and 5.28 (H-15, d, J = 7.0). The COSY spectrum indicated the presence of four isolated spin systems, C-1/C-2/C-3, C-6/C-7, C9/C-11/C-12, and C-14/C-15. Unambiguous assignment of all protons and their connectivities was achieved with the aid of HSQC and HMBC experiments. The carbonyl resonance at δ 169.4 ppm (C-19) was assigned through long-range correlations with H-18 and H_3-20 (Figure 1). A resonance at δ 2.17 was indicative of a methyl group at C-17, and the position of H_3-20 was confirmed by HMBC correlations with C-17, C-18, and C-19. HMBC correlations between H-14 and C-13, C-15, and C-16 confirmed the linkage between ring C and the lactone moiety (Figure 1A). Other key HMBC correlations were observed from Me-22 to C-7, C-8, and C- 9, from H_3-25 to C-10 and C-5, and from H_3-24 to C-4, C-5, and C-23. The UV spectrum showed a maximum at 274 nm and suggested an α,β,γ-unsaturated butenolide moiety.[17,18] Taken together, the NMR data of **1** were indicative of a sesterterpenoid, a class of terpenoids that has been reported from other *Salvia* species. The remaining degree of unsaturation was rationalized by the presence of an ether bridge connecting two quaternary carbon atoms (C-8 and C-13) in ring C. This was corroborated by the ^{13}C NMR chemical shift of C-8 (δ 76.9) and C-13 (δ 77.4). Hence, the

dx.doi.org/10.1021/np400948n | J. Nat. Prod. 2014, 77, 848−854

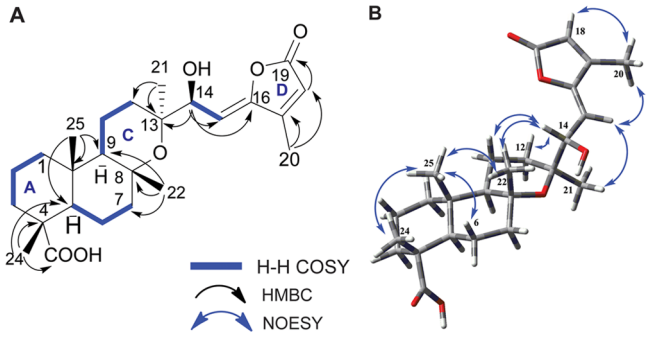

Figure 1. (A) Key HMBC correlations of **1** and (B) representation of key NOESY correlation.

available evidence indicated that **1** was a manoyloxide-type sesterterpenoid.

Considering the structure of compound **1**, a certain degree of conformational flexibility was expected for the pyran ring, with substituents at C-13 assuming either axial or equatorial orientations. In addition, rotation around the C-13/C-14 and C-14/C-15 bonds was to be expected. The relative configuration of the tricyclic ring was derived from coupling constants ($^3J_{H-H}$) and diagnostic NOESY correlations (Figure 1). In the NOESY spectrum, cross-peaks between H_3-25 (δ 0.89) and H_3-24 (δ 1.15), H-6β (δ 1.65), and H_3-22 (δ 1.40) confirmed that they were cofacial. The strong NOESY correlations between H-14 (δ 4.85) and H_3-22 (δ 1.40) suggested the α-orientation of H_3-21 (δ 1.12). Hence, the relative configuration of **1** was 4*R*,5*R*,8*R*,9*R*,10*S*,13*S*. The *Z*-geometry of the C-15−C-16 double bond was elucidated via the NOESY cross-peak between H-15 (δ 5.34) and H_3-20 (δ 2.17). The presence of an α,β,γ-unsaturated butenolide moiety adjacent to the C-13 and C-14 stereogenic centers suggested that the configuration at C-14 and, therefore, the absolute configuration of **1** could possibly be solved by ECD spectroscopy.

The ECD spectrum of **1** showed sequential positive and negative Cotton effects (CE) at 280 and 240 nm, respectively. Conformational analysis gave six conformers within a 2 kcal/mol energy window from the global minimum (Figure 2). The experimental

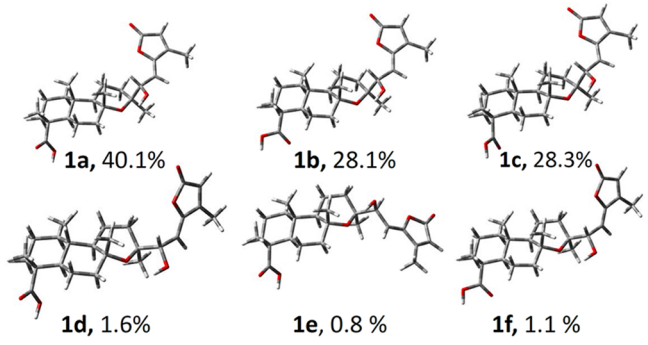

Figure 2. Energy-minimized conformers of **1** in the gas phase using DFT at the B3LYP/6-31G** level.

and the calculated ECD spectra obtained after Boltzmann weighting of the (13*S*,14*S*) and (13*S*,14*R*) stereoisomers are shown in Figure 3. The calculated ECD spectrum for the (13*S*,14*S*) stereoisomer showed excellent fit with the experimental data, with a positive CE around 280 nm (n → π^* transition) and a negative CE around 240 nm ($\pi \rightarrow \pi^*$ transition of the α,β,γ-unsaturated butenolide moiety). Thus, the absolute configuration

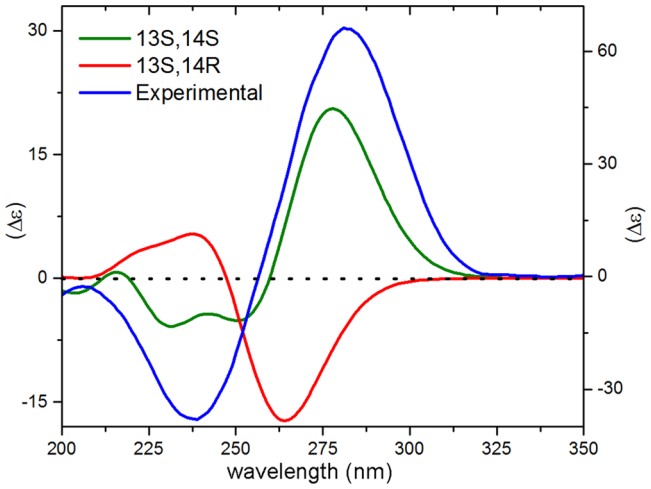

Figure 3. Comparison of experimental and calculated ECD spectra of **1** and the stereoisomers (13*S*,14*S*) and (13*S*,14*R*).

and the structure of compound **1** were established as (4*R*,5*R*,8*R*,9*R*,10*S*,13*S*,14*S*)-14-hydroxymanoyloxide-15,17-dien-15(*Z*)-16,19-olide. Compound **1** is a new sesterterpenoid, and the only second reported manoyloxide sesterterpenoid. Similar compounds had been previously found in *S. yosgadensis*,[17] but their absolute configuration had not been determined.

Compounds **2** and **3** had the same molecular formula, $C_{25}H_{36}O_6$, as **1**. Similar to **1**, the UV spectra of both compounds showed an absorption band at 273 nm for the α,β,γ-unsaturated butenolide moiety (Figure S16). The NMR spectroscopic data of **2** and **3** showed similarity to those of **1**, with small but diagnostic differences observed for some resonances in the ^{1}HNMR spectrum, e.g., for H-14 (δ 4.48 in **2** and 4.29 in **3**) and H_3-21 (δ 1.24 in **2** and 1.16 in **3**) (Table 1, Figure S14).

Compound **2** showed diagnostic NOESY correlations between H_3-25 (δ 0.82) and H-2β (δ 1.63), between H_3-21 (δ 1.29), H-12β (δ 1.82), H-14 (δ 4.29), and H-15 (δ 5.31), and between H-15 (δ_H 5.31) and H_3-20 (δ_H 2.16) (Figure 4), suggesting a relative configuration of 4*R*,5*R*,8*R*,9*R*,10*S*,13*R*. The absolute configuration of **2** was established by comparison of experimental and calculated ECD spectra for the (13*R*,14*R*) and (13*R*,14*S*) stereoisomers. The calculated ECD spectrum for the (13*R*,14*S*) stereoisomer showed an excellent fit with the experimental data (positive CE at 275 nm) (Figure 5), whereas the other stereoisomer showed a negative CE near 275 nm. The experimental ECD spectrum showed two positive CEs at 275 and 255 (shoulder) nm, which were due to the n → π^* transition of the α,β,γ-unsaturated butenolide moiety. Slight differences between the calculated and experimental data presumably resulted from minor differences between calculated and real conformers.[19] In conclusion, the structure of **2** was defined as (4*R*,5*R*,8*R*,9*R*,10*S*,13*R*,14*S*)-14-hydroxymanoyloxide-15,17-dien-15(*Z*)-16,19-olide.

NMR and ECD data indicated that compound **3** had to be a stereoisomer of **1** and **2**. The ^{1}H NMR chemical shifts of **3** were close to those of **2**, with differences for H-14, H-15, and H_3-21. The ECD spectrum of **3** showed a quasi-mirror image of that of compound **2** (Figure 6). However, **2** and **3** were not enantiomers, as they had been separated through non-enantioselective methods. Also, they showed diagnostic differences in their NMR spectra and specific rotations that were not opposite in sign. In the case of compound **3**, the NOESY spectrum did not permit an unequivocal assignment of the configuration at C-13.

dx.doi.org/10.1021/np400948n | *J. Nat. Prod.* 2014, 77, 848−854

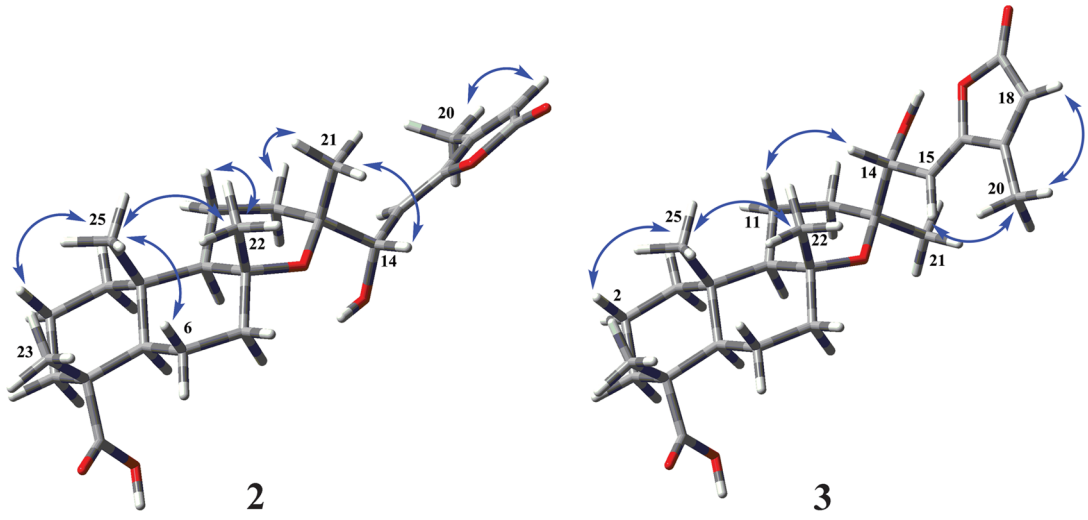

Figure 4. Lowest energy structures of **2** (left) and **3** (right) at the B3LYP/6-31G** level. The key NOESY correlations are specified by arrows.

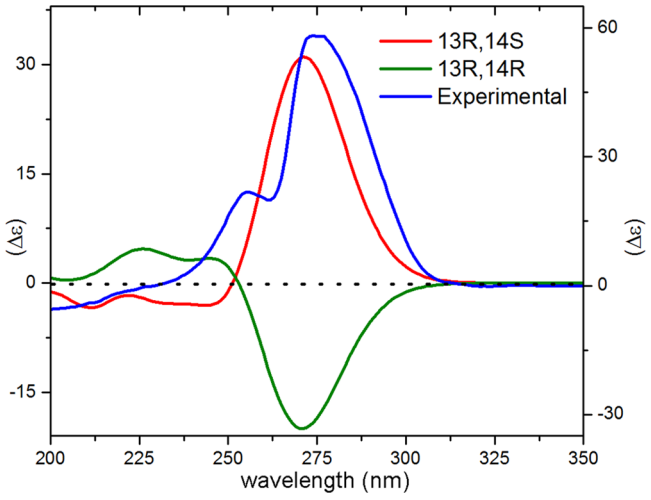

Figure 5. Comparison of the experimental ECD spectrum of **2** and calculated spectra of the (13*R*,14*S*) and (13*R*,14*R*) stereoisomers.

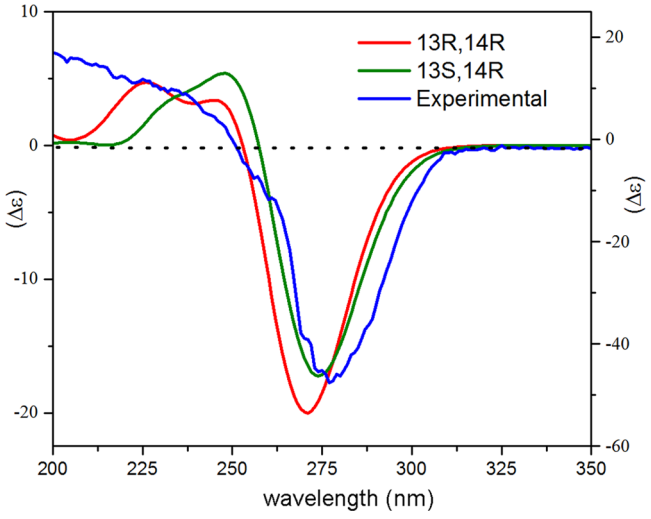

Figure 6. Comparison of the experimental ECD spectrum of **3** and calculated spectra of the (13*R*,14*R*) and (13*S*,14*R*) stereoisomers.

Therefore, the ECD spectra for the (13*R*,14*R*) and (13*S*,14*R*) stereoisomers were calculated (Figure 6). The spectrum of the (13*S*,14*R*) stereoisomer showed excellent fit with the experimental data, but the ECD spectrum of the 13*R*,14*R*-stereoisomer was too similar to unambiguously exclude it. Calculation of optical rotation has been successfully used for establishing the absolute configuration of natural products;[8,20] hence, the optical rotation values for both stereoisomers were calculated. The average $[\alpha]_D$ of the (13*S*,14*R*) and (13*R*,14*R*) stereoisomers were +5 and −70, respectively, while the experimental value was +1. Considering the good agreement between the calculated and experimental ECD spectra and optical rotation values, the structure of compound **3** was defined as (4*R*,5*R*,8*R*,9*R*,10*S*,13*S*,14*R*)-14-hydroxymanoyloxide-15,17-dien-15(*Z*)-16,19-olide.

For compound **4**, a molecular formula of $C_{25}H_{38}O_6$ was derived from ^{13}C NMR and HRESIMS ($[M + Na]^+$ ion at m/z 457.4560; calcd 457.2566). The molecular formula accounted for seven indices of hydrogen deficiency. The NMR data of **4** were similar to those of **1**−**3** (Tables 1 and 2). In particular, rings A−C appeared to be identical, and notable differences were observed only for resonances attributable to the C-13 side chain. In the ^{13}C NMR spectrum, the chemical shifts of C-15 and C-16 (δ 34.2 and 82.9, respectively) were indicative of the absence of an olefinic moiety, and the presence of an α,β-unsaturated butenolide was corroborated by the UV spectrum (λ_{max} at 222 nm). In the ^{1}HNMR spectrum, the vinylic H-18 appeared downfield at δ 5.71(s). In the COSY spectrum the resonances of H-16 (δ 5.03, d, J = 10.4 Hz) and H-14 (δ 3.75, d, J = 10.6 Hz) showed connectivities with H-15β (δ 1.58) and H-15α (δ 1.72) and thus belonged to the same spin system (C14−C15−C16). HMBC cross-peaks between H-14 and C-13, C-15, C-12, and C-16, and between H_3-20, C-16, C-17, and C-18 (Figure 7) corroborated the linkage of the side chain with the manoyloxide scaffold. The configuration of C-13 was assigned as *S* by 1D selective NOESY correlation between H_3-22 and H-14 (Figure S19), while the configurations of rings A and B were identical to those in **1**−**3**. With respect to the C-14 and C-16 configurations, four stereoisomers, (13*S*,14*S*,16*S*), (13*S*,14*R*,16*S*), (13*S*,14*S*,16*R*), and (13*S*,14*R*,16*R*), were possible. The experimental ECD spectrum of **4** (Figure 8) showed sequential positive and negative CEs around 215−235 nm (n → π^* transition) and 200−210 nm ($\pi \rightarrow \pi^*$ transition), respectively. These CEs indicated a left-handed helicity (*M*) of the α,β-unsaturated butenolide ring and, therefore, an *R* configuration of C-16.[21,22] However, due to high conformational flexibility and free rotation around C-14/C-15, we could not

dx.doi.org/10.1021/np400948n | J. Nat. Prod. 2014, 77, 848−854

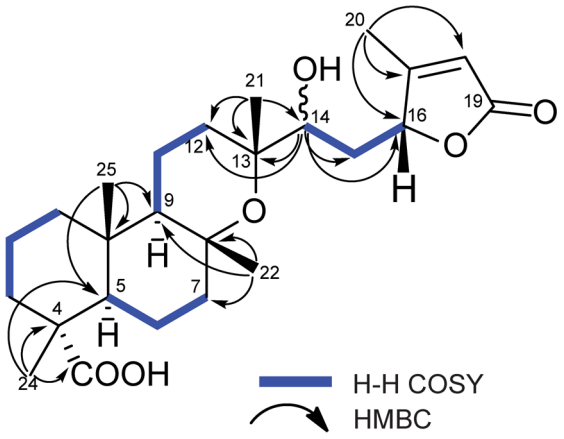

Figure 7. Key HMBC correlations of **4**.

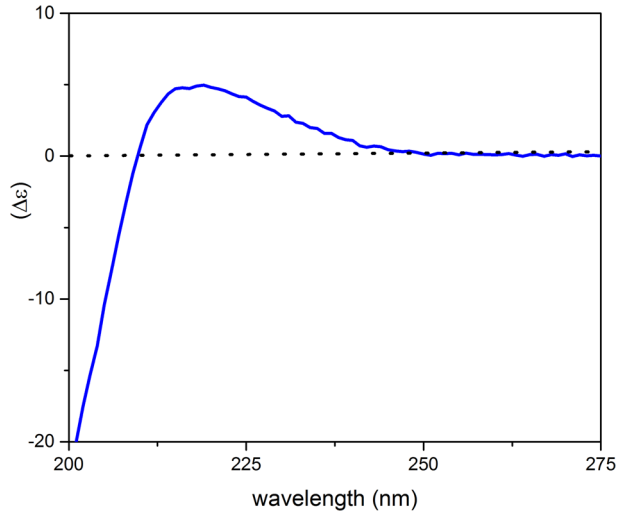

Figure 8. Experimental ECD spectrum of **4**.

determine the configuration at C-14. Hence, the structure of **4** was established as (4*R*,5*R*,8*R*,9*R*,10*S*,13*S*,16*R*)-14-hydroxymanoyloxide-17-en-16,19-olide.

A molecular formula of $C_{25}H_{36}O_5$ for compound **5** was deduced from ^{13}C NMR and HRESIMS data (*m*/*z* 439.2452 $[M + Na]^+$ ion, calcd 439.2460). NMR data indicated a close structural similarity to compounds **1**−**3**. A notable difference in the ^{1}HNMR spectrum was the lack of an oxygenated methine (H-14) and the presence of two diastereotopic methylene protons at δ 2.79 (H-14β) and 2.52 (H-14*a*). The COSY spectrum showed diagnostic cross-peaks between H-14 (a and b) and H-15 and between H-18 and H_3-20. HMBC connectivities between H-15, C-13 (δ 73.4), and C-16, and between H-14, C-16, C-15, C-13, and C-21 confirmed the linkage of the two portions of the molecule. The relative configuration of rings A−C was established via NOESY data. A UV absorption band at 273 nm corroborated the presence of an α,β,γ-unsaturated butenolide moiety. The ECD spectrum showed a positive CE at 290 nm (n → π^* transition) and a negative CE at 235 nm ($\pi \rightarrow \pi^*$ transition of an α,β,γ-unsaturated butenolide). The calculated ECD spectrum of the (4*R*,5*R*,8*R*,9*R*,10*S*,13*R*)-stereoisomer showed a strong positive CE at 290 nm, which fitted well with the experimental data (Figure 9). However, the negative CE at 230 nm in the experimental spectrum was absent in the calculated spectrum. Therefore, the ECD spectrum for the

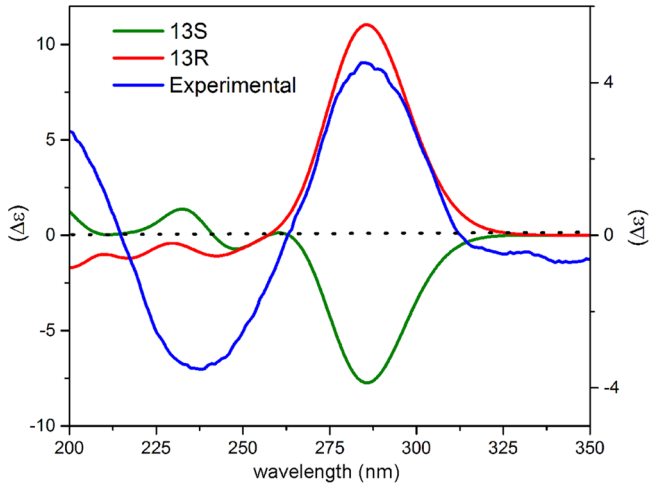

Figure 9. Comparison of experimental and calculated ECD spectra of **5**.

(4*R*,5*R*,8*R*,9*R*,10*S*,13*S*)-stereoisomer (Figure 9) was calculated but showed a negative CE at 290 nm. For confirmation the optical rotation for both stereoisomers was also calculated and compared with experimental data. The average $[\alpha]_D$ values of the (13*S*) and (13*R*) stereoisomers were +27 and +112, respectively, while the experimental value was +90. Hence, we concluded that the structure of **5** was (4*R*,5*R*,8*R*,9*R*,10*S*,13*R*)-manoyloxide-15,17-dien-15(*Z*)-16,19-olide.

Salvia is thus far the only genus in the Lamiaceae family that contains sesterterpenes, and they have been typically found in the aerial parts of the plants. Salvia species of the Middle East, such as *S. hypoleuca*,[13] *S. sahendica*,[14,15] *S. mirzayanii*,[16] *S. dominica*,[11] *S. yosgadensis*,[17] and *S. palaestina*,[18] are rich sources for this class of compounds. Thus far, mainly labdane-type sesterterpenes have been reported, and manoyloxide derivatives have been reported only from *S. yosgadensis*.[17] Hence, this is only the second report on the characterization of manoyloxide-type sesterterpenes from nature, and the first study where their absolute configuration was established by comparison of experimental and calculated ECD spectra and optical rotation values.

EXPERIMENTAL SECTION

General Experimental Procedures. Optical rotations were measured using a JASCO P-2000 automatic digital polarimeter. NMR spectra were recorded at 18 °C on a Bruker Avance III 500 MHz spectrometer operating at 500.13 MHz for ^{1}H and 125.77 MHz for ^{13}C. A 1 mm TXI microprobe with *z*-gradient was used for ^{1}H-detected experiments. ^{13}C NMR spectra were recorded with a 5 mm BBO probehead with *z*-gradient. Spectra were analyzed using Bruker TopSpin 2.1 software. $CDCl_3$ and methanol-d_4 for NMR were purchased from Armar Chemicals. ECD spectra were recorded in MeOH with a Chirascan CD spectrometer. HRESIMS in positive mode were recorded on a Bruker microTOF ESIMS system with a scan range of *m*/*z* 150−1500.

The preparative HPLC system consisted of a Shimadzu SCL-10VP controller and binary pump (LC-8A), UV−vis SPD-M10A VP detector, and Class-VP 6.12 software. An aliquot of the sample was dissolved in DMSO (100 mg/mL) and separated by preparative HPLC column (SunFire C_{18}, 5 μm, 30 × 150.0 mm i.d.; Waters) using a linear gradient of H_2O−MeCN (both containing 0.1% formic acid), 40:60 → 0:100 in 30 min. The flow rate was 20 mL/min, and detection was at 280 nm. Aliquots of 200 μL of sample solutions were injected.

Plant Material. The aerial parts of *Salvia mirzayanii* were collected in March 2011 on Genu Mountain in the Bandar Abbas area of Southern Iran. The plant material identified by Mr. Soltanipoor, Agricultural and Natural Resources Center of Hormozgan, Bandar Abbas, Iran, and a

dx.doi.org/10.1021/np400948n | J. Nat. Prod. 2014, 77, 848−854

voucher specimen (5322) have been deposited in the herbarium of ANRC.

Extraction and Isolation. The dried plant material (4.5 kg) was ground and extracted by maceration with *n*-hexane (5 × 25 L), acetone (5 × 25 L), and MeOH (5 × 25 L). Evaporation of the acetone extract afforded 125 g of a dark gummy residue. The extract was separated on a silica gel column (230−400 mesh, 127.0 × 5.0 cm, 750 g) with a gradient of *n*-hexane−EtOAc (100:0 to 0:100) as eluent, followed by increasing concentrations of MeOH (up to 25%) in EtOAc. Fractions of 250 mL were collected and pooled on the basis of TLC analysis. A total of 30 fractions were obtained. The early eluting fractions contained waxes and carotenoids and were not further investigated. Fraction 15 (4.5 g, eluted with *n*-hexane−EtOAc (55:45)) was subjected to silica gel column chromatography (70−230 mesh, 3.5 × 55.0 cm, 210 g). Separation with acetone−$CHCl_3$ (7:93) afforded two fractions (15P and 15K). An aliquot of 15P (100 mg) was separated by preparative HPLC (SunFire C18, 5 μm, 30 × 150.0 mm i.d.; Waters) with the following gradient: H_2O−MeCN, isocratic 60:40 for 5 min; 60:40 → 50:50 in 7 min; isocratic with 50:50 for 6 min; 50:40 in 12 min. The flow rate was 20 mL/min, and detection was at 280 nm. Fraction 15P was dissolved in DMSO at a concentration of 100 mg/mL, and aliquots of 330 μL were injected. Fraction 15P afforded **1** (7.3 mg, t_R = 21.0 min, >95% purity [^{1}HNMR]), **2** (6.6 mg, t_R = 25.0 min, >95% purity [^{1}HNMR]), and **3** (6.0 mg, t_R = 27.0 min, >95% purity [^{1}HNMR]). Fraction 21 (eluted with *n*-hexane−EtOAc (40:60)) afforded a crude solid, which was triturated with acetone to separate the insoluble part, from which compound **4** was obtained as an amorphous solid (14 mg, >95% purity [^{1}HNMR]). Purification of a portion of fraction 11 (80 mg) by preparative RP-HPLC (same mobile gradient profile as above) afforded **5** (6.2 mg, t_R = 27.0 min, >95% purity [^{1}HNMR]).

Computational Methods. Conformation analysis of **1**−**3** and **5** was performed with Schrödinger MacroModel 9.1 (Schrödinger, LLC, New York) employing the OPLS2005 (optimized potential for liquid simulations) force field in H_2O. Conformers within a 2 kcal/mol energy window from the global minimum were selected for geometrical optimization and energy calculation applying DFT with Becke's nonlocal three-parameter exchange and correlation functional and the Lee−Yang−Parr correlation functional level (B3LYP) using the 6-31G** basis set in the gas phase with the Gaussian 09 program package.[23] Vibrational evaluation was done at the same level to confirm minima. Excitation energy (denoted by wavelength in nm), rotatory strength dipole velocity (R_{vel}), and dipole length (R_{len}) were calculated in MeOH by TD-DFT/CAM-B3LYP/6-31G**, using the SCRF method, with the CPCM model. ECD curves were obtained on the basis of rotatory strengths with a half-band of 0.3 eV using SpecDis v1.61.[24] The OR calculations were carried out with TDDFT/GIAO methodology using CAM-B3LYP/6-31G** in $CHCl_3$ (SCRF/CPCM). The ECD spectra and optical rotation values were calculated from the spectra of individual conformers according to their contribution to Boltzmann weighting.

(4*R*,5*R*,8*R*,9*R*,10*S*,13*S*,14*S*)-14-Hydroxymanoyloxide-15,17-dien-15(*Z*)-16,19-olide (1): white powder; $[\alpha]_D^{25}$ +40 (*c* 0.8, $CHCl_3$); for ^{1}H and ^{13}C NMR data, see Tables 1 and 2; UV (MeOH) λ_{max} (log ε) 274 (2.7); ECD (MeOH, *c* 0.07 mM, 0.1 cm) $[\theta]_{236}$ = −121 211, $[\theta]_{281}$ = +207 966; HRESITOFMS *m*/*z* 455.2399 [M + Na]$^+$, calcd for $C_{25}H_{36}O_6Na$, 455.2410.

(4*R*,5*R*,8*R*,9*R*,10*S*,13*R*,14*S*)-14-Hydroxymanoyloxide-15,17-dien-15(*Z*)-16,19-olide (2): white powder; $[\alpha]_D^{25}$ +51 (*c* 0.8, $CHCl_3$); for ^{1}H and ^{13}C NMR data, see Tables 1 and 2; UV (MeOH) λ_{max} (log ε) 274 (4.3), 256 (2.85); ECD (MeOH, *c* 0.07 mM, 0.1 cm) $[\theta]_{274}$ = +360 167, $[\theta]_{256}$ = +142 864 (shoulder); HRESITOFMS *m*/*z* 455.2404 [M + Na]$^+$, calcd for $C_{25}H_{36}O_6Na$, 455.2410.

(4*R*,5*R*,8*R*,9*R*,10*S*,13*S*,14*R*)-14-Hydroxymanoyloxide-15,17-dien-15(*Z*)-16,19-olide (3): white powder; $[\alpha]_D^{25}$ +1 (*c* 0.8, $CHCl_3$); for ^{1}H and ^{13}C NMR data, see Tables 1 and 2; UV (MeOH) λ_{max} (log ε) 274 (3.1); ECD (MeOH, *c* 0.07 mM, 0.1 cm) $[\theta]_{274}$ = −152 580; HRESITOFMS *m*/*z* 455.2404 [M + Na]$^+$, calcd for $C_{25}H_{36}O_6Na$, 455.2410.

(4*R*,5*R*,8*R*,9*R*,10*S*,13*S*,16*R*)-14-Hydroxymanoyloxide-17-en-16,19-olide (4): white powder; $[\alpha]_D^{25}$ = +6 (*c* 0.8, $CHCl_3$); for ^{1}H and ^{13}C NMR data, see Tables 1 and 2; UV (MeOH) λ_{max} (log ε) 222 (4.72); ECD (MeOH, *c*1.0 mM, 0.1 cm) $[\theta]_{202}$ = −17 103, $[\theta]_{218}$ = +4799; HRESITOFMS *m*/*z* 457.2560 [M + Na]$^+$, calcd for $C_{25}H_{38}O_6Na$, 457.2566.

(4*R*,5*R*,8*R*,9*R*,10*S*,13*R*)-Manoyloxide-15,17-dien-15(*Z*)-16,19-olide (5): white powder; $[\alpha]_D^{25}$ +90 (*c* 0.8, $CHCl_3$); for ^{1}H and ^{13}C NMR data, see Tables 1 and 2; UV (MeOH) λ_{max} (log ε) 273 (4.72); ECD (MeOH, *c* 1.0 mM, 0.1 cm) $[\theta]_{232}$ = −1850, $[\theta]_{290}$ = +2491; HRESITOFMS *m*/*z* 439.2452 [M + Na]$^+$, calcd for $C_{25}H_{36}O_5Na$, 439.2460.

■ ASSOCIATED CONTENT

Ⓢ Supporting Information

1D and 2D NMR spectra, minimized structures, and calculated ECD spectra of conformers of **1**−**5** can be found as Supporting Information. This material is available free of chharge via the Internet at http://pubs.acs.org.

■ AUTHOR INFORMATION

Corresponding Authors

*E-mail: m_moridi@sbu.ac.ir.

*Tel: +41-61-2671425. Fax: +41-61-2671474. E-mail: matthias.hamburger@unibas.ch.

Author Contributions

⊥S. N. Ebrahimi and M. M. Farimani contributed equally to this work.

Notes

The authors declare no competing financial interest.

■ ACKNOWLEDGMENTS

Financial support by the Shahid Beheshti University Research Council (to M.M.F.) and by the Swiss National Science Foundation (Project 31600-113109, to M.H.) is gratefully acknowledged. We thank Dr. T. Sharpe (Biozentrum, University of Basel) for technical assistance with measurement of UV and ECD spectra.

■ REFERENCES

(1) Wu, Y. B.; Ni, Z. Y.; Shi, Q. W.; Dong, M.; Kiyota, H.; Gu, Y. C.; Cong, B. *Chem. Rev.* **2012**, *112*, 5967−6026.

(2) Mozaffarian, V. *A Dictionary of Iranian Plant Names*; Farhang Moaser: Tehran, 1996; Vol. 3.

(3) Rustaiyan, A.; Masoudi, S.; Tabatabaei-Anaraki, M. *Nat. Prod. Commun.* **2007**, *2*, 1031−1042.

(4) Habibi, Z.; Eftekhar, F.; Samiee, K.; Rustaiyan, A. *J. Nat. Prod.* **2000**, *63*, 270−271.

(5) Jassbi, A. R.; Mehrdad, M.; Eghtesadi, F.; Ebrahimi, S. N.; Baldwin, I. T. *Chem. Biodiversity* **2006**, *3*, 916−922.

(6) Salehi, P.; Sonboli, A.; Ebrahimi, S. N.; Yousefzadi, M. *Chem. Nat. Compd.* **2007**, *43*, 328−330.

(7) Farimani, M. M.; Taheri, S.; Ebrahimi, S. N.; Bahadori, M. B.; Khavasi, H. R.; Zimmermann, S.; Brun, R.; Hamburger, M. *Org. Lett.* **2011**, *14*, 166−169.

(8) Ebrahimi, S. N.; Zimmermann, S.; Zaugg, J.; Smiesko, M.; Brun, R.; Hamburger, M. *Planta Med.* **2013**, *79*, 150−156.

(9) Farimani, M. M.; Ebrahimi, S. N.; Salehi, P.; Bahadori, M. B.; Sonboli, A.; Khavasi, H. R.; Zimmermann, S.; Kaiser, M.; Hamburger, M. *J. Nat. Prod.* **2013**, *76*, 1806−1809.

(10) Cioffi, G.; Bader, A.; Malafronte, A.; Dal Piaz, F.; De Tommasi, N. *Phytochemistry* **2008**, *69*, 1005−1012.

(11) Dal Piaz, F.; Vassallo, A.; Lepore, L.; Tosco, A.; Bader, A.; De Tommasi, N. *J. Med. Chem.* **2009**, *52*, 3814−3828.

(12) Wang, L.; Yang, B.; Lin, X.-P.; Zhou, X.-F.; Liu, Y. *Nat. Prod. Rep.* **2013**, *30*, 455−473.

(13) Rustaiyan, A.; Koussari, S. *Phytochemistry* **1988**, *27*, 1767−1769.

(14) Linden, A.; Juch, M.; Moghaddam, F. M.; Zaynizadeh, B.; Ruedi, P. *Phytochemistry* **1996**, *41*, 589−590.

(15) Moghaddam, F. M.; Farimani, M. M.; Seirafi, M.; Taheri, S.; Khavasi, H. R.; Sendker, J.; Proksch, P.; Wray, V.; Edrada, R. *J. Nat. Prod.* **2010**, *73*, 1601−1605.
(16) Moghaddam, F. M.; Amiri, R.; Alam, M.; Hossain, M. B.; van der Helm, D. *J. Nat. Prod.* **1998**, *61*, 279−281.
(17) Topcu, G.; Ulubelen, A.; Tam, T. C. M.; TaoChe, C. *Phytochemistry* **1996**, *42*, 1089−1092.
(18) Cioffi, G.; Bader, A.; Malafronte, A.; Dal Piaz, F.; De Tommasi, N. *Phytochemistry* **2008**, *69*, 1005−1012.
(19) Zaugg, J.; Ebrahimi, S. N.; Smiesko, M.; Baburin, I.; Hering, S.; Hamburger, M. *Phytochemistry* **2011**, *72*, 2385−2395.
(20) Stephens, P. J.; Pan, J. J.; Devlin, F. J.; Cheeseman, J. R. *J. Nat. Prod.* **2008**, *71*, 285−288.
(21) Kamel, H. N.; Ding, Y.; Li, X. C.; Ferreira, D.; Fronczek, F. R.; Slattery, M. *J. Nat. Prod.* **2009**, *72*, 900−905.
(22) Gawronski, J. K.; van Oeveren, A.; van der Deen, H.; Leung, C. W.; Feringa, B. L. *J. Org. Chem.* **1996**, *61*, 1513−1515.
(23) Frisch, M. J.; Trucks, G. W.; Schlegel, H. B.; Scuseria, G. E.; Robb, M. A.; Cheeseman, J. R.; Scalmani, G.; Barone, V.; Mennucci, B.; Petersson, G. A.; Nakatsuji, H.; Caricato, M.; Li, X.; Hratchian, H. P.; Izmaylov, A. F.; Bloino, J.; Zheng, G.; Sonnenberg, J. L.; Hada, M.; Ehara, M.; Toyota, K.; Fukuda, R.; Hasegawa, J.; Ishida, M.; Nakajima, T.; Honda, Y.; Kitao, O.; Nakai, H.; Vreven, T.; Montgomery, J. A.; Peralta, J. E.; Ogliaro, F.; Bearpark, M.; Heyd, J. J.; Brothers, E.; Kudin, K. N.; Staroverov, V. N.; Kobayashi, R.; Normand, J.; Raghavachari, K.; Rendell, A.; Burant, J. C.; Iyengar, S. S.; Tomasi, J.; Cossi, M.; Rega, N.; Millam, J. M.; Klene, M.; Knox, J. E.; Cross, J. B.; Bakken, V.; Adamo, C.; Jaramillo, J.; Gomperts, R.; Stratmann, R. E.; Yazyev, O.; Austin, A. J.; Cammi, R.; Pomelli, C.; Ochterski, J. W.; Martin, R. L.; Morokuma, K.; Zakrzewski, V. G.; Voth, G. A.; Salvador, P.; Dannenberg, J. J.; Dapprich, S.; Daniels, A. D.; Farkas, O.; Foresman, J. B.; Ortiz, J. V.; Cioslowski, J.; Fox, D. J. *Gaussian 09*, Revision A02; Gaussian, Inc: Wallingford, CT, 2009.
(24) Bruhn, T.; Schaumlöffel, A.; Hemberger, Y.; Bringmann, G. *SpecDis* version 1.61; University of Wuerzburg: Germany, 2013.